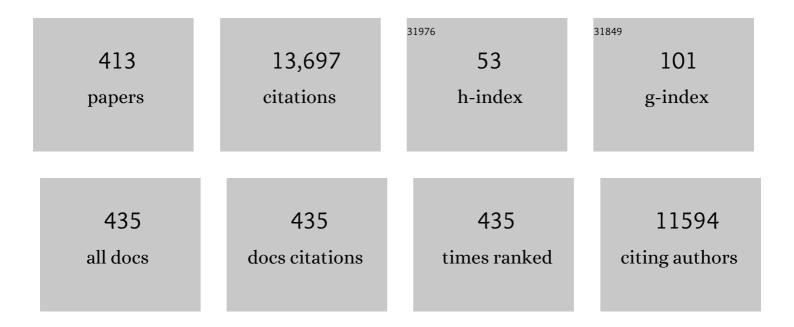
List of Publications by Year in descending order

Source: https://exaly.com/author-pdf/7697020/publications.pdf Version: 2024-02-01



#	Article	IF	CITATIONS
1	Highly Efficient Water Splitting into H2and O2over Lanthanum-Doped NaTaO3Photocatalysts with High Crystallinity and Surface Nanostructure. Journal of the American Chemical Society, 2003, 125, 3082-3089.	13.7	1,585
2	Alkaliâ€Metalâ€Promoted Pt/TiO ₂ Opens a More Efficient Pathway to Formaldehyde Oxidation at Ambient Temperatures. Angewandte Chemie - International Edition, 2012, 51, 9628-9632.	13.8	611
3	Catalytic activity and structural analysis of polymer-protected gold-palladium bimetallic clusters prepared by the simultaneous reduction of hydrogen tetrachloroaurate and palladium dichloride. The Journal of Physical Chemistry, 1992, 96, 9927-9933.	2.9	343
4	Structural analysis of polymer-protected palladium/platinum bimetallic clusters as dispersed catalysts by using extended x-ray absorption fine structure spectroscopy. The Journal of Physical Chemistry, 1991, 95, 7448-7453.	2.9	310
5	Polymer-Protected Ni/Pd Bimetallic Nano-Clusters:Â Preparation, Characterization and Catalysis for Hydrogenation of Nitrobenzene. Journal of Physical Chemistry B, 1999, 103, 9673-9682.	2.6	279
6	Nickel-loaded K4Nb6O17 photocatalyst in the decomposition of H2O into H2 and O2: Structure and reaction mechanism. Journal of Catalysis, 1989, 120, 337-352.	6.2	278
7	Active Oxygen Species and Mechanism for Low-Temperature CO Oxidation Reaction on a TiO2-Supported Au Catalyst Prepared from Au(PPh3)(NO3) and As-Precipitated Titanium Hydroxide. Journal of Catalysis, 1999, 185, 252-264.	6.2	275
8	Influence of sulfation on iron titanate catalyst for the selective catalytic reduction of NOx with NH3. Applied Catalysis B: Environmental, 2011, 103, 369-377.	20.2	245
9	Electron Transfer Effects in Ozone Decomposition on Supported Manganese Oxide. Journal of Physical Chemistry B, 2001, 105, 4245-4253.	2.6	179
10	Polarized Cu K-edge XANES of square planar CuCl42â^' ion. Experimental and theoretical evidence for shake-down phenomena. Chemical Physics, 1984, 91, 249-256.	1.9	172
11	Supported Au Catalysts Prepared from Au Phosphine Complexes and As-Precipitated Metal Hydroxides: Characterization and Low-Temperature CO Oxidation. Journal of Catalysis, 1997, 170, 191-199.	6.2	166
12	Ni@NiO Core–Shell Structure-Modified Nitrogen-Doped InTaO ₄ for Solar-Driven Highly Efficient CO ₂ Reduction to Methanol. Journal of Physical Chemistry C, 2011, 115, 10180-10186.	3.1	165
13	Catalytic activity and structural analysis of polymer-protected gold/palladium bimetallic clusters prepared by the successive reduction of hydrogen tetrachloroaurate(III) and palladium dichloride. The Journal of Physical Chemistry, 1993, 97, 5103-5114.	2.9	163
14	An Al-doped SrTiO ₃ photocatalyst maintaining sunlight-driven overall water splitting activity for over 1000Âh of constant illumination. Chemical Science, 2019, 10, 3196-3201.	7.4	163
15	Highly dispersed iron vanadate catalyst supported on TiO2 for the selective catalytic reduction of NOx with NH3. Journal of Catalysis, 2013, 307, 340-351.	6.2	149
16	Effects of Boundaries on Pattern Formation: Catalytic Oxidation of CO on Platinum. Science, 1994, 264, 80-82.	12.6	145
17	Interconvertible multiple photoluminescence color of a gold(<scp>i</scp>) isocyanide complex in the solid state: solvent-induced blue-shifted and mechano-responsive red-shifted photoluminescence. Chemical Science, 2015, 6, 2187-2195.	7.4	133
18	Photocatalytic O ₂ Evolution of Rhodium and Antimony-Codoped Rutile-Type TiO ₂ under Visible Light Irradiation. Journal of Physical Chemistry C, 2007, 111, 17420-17426.	3.1	128

#	Article	IF	CITATIONS
19	Reactant-promoted reaction mechanism for catalytic water-gas shift reaction on MgO. Journal of Catalysis, 1990, 122, 55-67.	6.2	125
20	Silver-modulated SiO2-supported copper catalysts for selective hydrogenation of dimethyl oxalate to ethylene glycol. Journal of Catalysis, 2013, 307, 74-83.	6.2	123
21	Variability in the Structure of Supported MoO3 Catalysts:  Studies Using Raman and X-ray Absorption Spectroscopy with ab Initio Calculations. Journal of Physical Chemistry B, 2001, 105, 8519-8530.	2.6	121
22	Co Single Atoms in ZrO ₂ with Inherent Oxygen Vacancies for Selective Hydrogenation of CO ₂ to CO. ACS Catalysis, 2021, 11, 9450-9461.	11.2	116
23	Photocatalytic activity and reaction mechanism of Pt-intercalated K4Nb6O17 catalyst on the water splitting in carbonate salt aqueous solution. Journal of Photochemistry and Photobiology A: Chemistry, 1998, 114, 125-135.	3.9	107
24	Structural analysis of polymer-protected platinum/rhodium bimetallic clusters using extended x-ray absorption fine structure spectroscopy. Importance of microclusters for the formation of bimetallic clusters. The Journal of Physical Chemistry, 1994, 98, 2653-2662.	2.9	106
25	Influence of calcination temperature on iron titanate catalyst for the selective catalytic reduction of NOx with NH3. Catalysis Today, 2011, 164, 520-527.	4.4	98
26	Subsurface oxygen on Pt(100): kinetics of the transition from chemisorbed to subsurface state and its reaction with CO, H2 and O2. Surface Science, 1994, 313, 52-63.	1.9	95
27	Remarkable enhancement of Cu catalyst activity in hydrogenation of dimethyl oxalate to ethylene glycol using gold. Catalysis Science and Technology, 2012, 2, 1637.	4.1	95
28	Characterization and Kinetic Studies on the Highly Active Ammoxidation Catalyst MoVNbTeOx. Journal of Catalysis, 2000, 194, 309-317.	6.2	87
29	Structure of polymer-protected palladium-platinum bimetallic clusters at the oxidized state: extended x-ray absorption fine structure analysis. The Journal of Physical Chemistry, 1992, 96, 9730-9738.	2.9	86
30	Structure and catalytic combustion activity of atomically dispersed Pt species at MgO surface. Applied Catalysis A: General, 1999, 188, 313-324.	4.3	86
31	Carbon Nanotube-Supported RuFe Bimetallic Nanoparticles as Efficient and Robust Catalysts for Aqueous-Phase Selective Hydrogenolysis of Glycerol to Glycols. ACS Catalysis, 2011, 1, 1521-1528.	11.2	83
32	EXAFS measurements of a working catalyst in the liquid phase: An in situ study of a Ni2P hydrodesulfurization catalyst. Journal of Catalysis, 2006, 241, 20-24.	6.2	81
33	Iron-Oxide Supported Gold Catalysts Derived from Gold-Phosphine Complex Au(PPh3)(NO3): State and Structure of the Support. Journal of Catalysis, 1998, 176, 426-438.	6.2	78
34	Exploring the catalytic properties of supported palladium catalysts in the transfer hydrogenolysis of glycerol. Applied Catalysis B: Environmental, 2015, 166-167, 121-131.	20.2	76
35	Rheniumâ€Loaded TiO ₂ : A Highly Versatile and Chemoselective Catalyst for the Hydrogenation of Carboxylic Acid Derivatives and the Nâ€Methylation of Amines Using H ₂ and CO ₂ . Chemistry - A European Journal, 2017, 23, 14848-14859.	3.3	76
36	Preparation of supported gold catalysts from gold complexes and their catalytic activities for CO oxidation. Catalysis Letters, 1996, 42, 15-20.	2.6	75

#	Article	IF	CITATIONS
37	Metal-assisted hydroformylation on a SiO2-attached rhodium dimer. In situ EXAFS and FT-IR observations of the dynamic behaviors of the dimer site. Journal of the American Chemical Society, 1990, 112, 9096-9104.	13.7	74
38	In situ FTIR and XANES studies of thiophene hydrodesulfurization on Ni2P/MCM-41. Journal of Catalysis, 2009, 268, 209-222.	6.2	73
39	Unprecedented selectivity to the direct desulfurization (DDS) pathway in a highly active FeNi bimetallic phosphide catalyst. Journal of Catalysis, 2012, 285, 1-5.	6.2	73
40	Design and Characterization by EXAFS, FTIR, and TEM of Rh-Sn/SiO2 Catalysts Active for NO-H2 Reaction. Journal of Catalysis, 1994, 149, 70-80.	6.2	67
41	Controlling the Length and Shape of Gold Nanorods. Journal of Physical Chemistry B, 2005, 109, 19553-19555.	2.6	67
42	Supported Gold Catalysts Prepared from a Gold Phosphine Precursor and As-Precipitated Metal-Hydroxide Precursors: Effect of Preparation Conditions on the Catalytic Performance. Journal of Catalysis, 2000, 196, 56-65.	6.2	66
43	Polarized Total-Reflection Fluorescence EXAFS Study of Anisotropic Structure Analysis for Co Oxides on α-Al2O3 (0001) as Model Surfaces for Active Oxidation Catalysts. Journal of Catalysis, 1994, 145, 159-165.	6.2	64
44	Catalysis on microstructured surfaces: Pattern formation during CO oxidation in complex Pt domains. Physical Review E, 1995, 52, 76-93.	2.1	63
45	Evidence of Nonelectrochemical Shift Reaction on a CO-Tolerant High-Entropy State Pt–Ru Anode Catalyst for Reliable and Efficient Residential Fuel Cell Systems. Journal of the American Chemical Society, 2012, 134, 14508-14512.	13.7	63
46	New SiO2-supported niobium monomer catalysts for dehydrogenation of ethanol. Journal of the Chemical Society Chemical Communications, 1986, , 1660.	2.0	59
47	A new method for quantitative characterization of adsorbed hydrogen on Pt particles by means of Pt L-edge XANES. Chemical Physics Letters, 1996, 256, 445-448.	2.6	57
48	Supported gold catalysis derived from the interaction of a Au–phosphine complex with as-precipitated titanium hydroxide and titanium oxide. Catalysis Today, 1998, 44, 333-342.	4.4	57
49	Study of Gold Species in Iron-Oxide-Supported Gold Catalysts Derived from Gold-Phosphine Complex Au(PPh3)(NO3) and As-Precipitated Wet Fe(OH)3*. Journal of Catalysis, 1999, 181, 37-48.	6.2	57
50	Dynamic Behaviour of Active Sites of a SiO ₂ -Attached Mo(VI)-Dimer Catalyst during Ethanol Oxidation Observed by Means of EXAFS. Zeitschrift Fur Physikalische Chemie, 1985, 144, 105-115.	2.8	56
51	Structure and behaviour of Ru3(CO)12 supported on inorganic oxide surfaces, studied by EXAFS, infrared spectroscopy and temperature-programmed decomposition. Journal of the Chemical Society, Faraday Transactions, 1990, 86, 2645.	1.7	54
52	Synthesis, characterization, and catalytic properties of silica-attached one-atomic-layer niobium oxide catalysts. The Journal of Physical Chemistry, 1991, 95, 1711-1716.	2.9	53
53	Polarization-Dependent Total-Reflection Fluorescence XAFS Study of Mo Oxides on a Rutile TiO2(110) Single Crystal Surface. Journal of Physical Chemistry B, 1998, 102, 9006-9014.	2.6	53
54	Characterization of Pt-doped SnO2 catalyst for a high-performance micro gas sensor. Physical Chemistry Chemical Physics, 2013, 15, 17938.	2.8	53

#	Article	IF	CITATIONS
55	<i>In Situ</i> X-ray Absorption Fine Structure Analysis of PtCo, PtCu, and PtNi Alloy Electrocatalysts: The Correlation of Enhanced Oxygen Reduction Reaction Activity and Structure. Journal of Physical Chemistry C, 2016, 120, 11519-11527.	3.1	53
56	The First Atomic-scale Observation of a Ni2P(0001) Single Crystal Surface. Chemistry Letters, 2006, 35, 90-91.	1.3	52
57	Combined in situ QXAFS and FTIR analysis of a Ni phosphide catalyst under hydrodesulfurization conditions. Journal of Catalysis, 2012, 286, 165-171.	6.2	52
58	In-Situ Polarization-Dependent Total-Reflection Fluorescence XAFS Studies on the Structure Transformation of Pt Clusters on α-Al2O3(0001). Journal of Physical Chemistry B, 1997, 101, 5549-5556.	2.6	51
59	Structure of MnOx/Al2O3 Catalyst:  A Study Using EXAFS, In Situ Laser Raman Spectroscopy and ab Initio Calculations. Journal of Physical Chemistry B, 2001, 105, 9067-9070.	2.6	51
60	Ultrathin inorganic molecular nanowire based on polyoxometalates. Nature Communications, 2015, 6, 7731.	12.8	50
61	Characterization of the Structure of RuO2â^'IrO2/Ti Electrodes by EXAFS. Journal of Physical Chemistry B, 1998, 102, 3736-3741.	2.6	49
62	Time-resolved DXAFS study on the reduction processes of Cu cations in ZSM-5. Catalysis Letters, 2000, 68, 139-145.	2.6	48
63	Control of Reactivity in Câ^'H Bond Breaking Reactions on Oxide Catalysts:Â Methanol Oxidation on Supported Molybdenum Oxide. Journal of Physical Chemistry B, 2003, 107, 1845-1852.	2.6	48
64	X-ray absorption fine structure (XAFS) analyses of Ni species trapped in graphene sheet of carbon nanofibers. Physical Review B, 2006, 73, .	3.2	48
65	Synthesis of Silica-Supported Compact Phosphines and Their Application to Rhodium-Catalyzed Hydrosilylation of Hindered Ketones with Triorganosilanes. Organometallics, 2008, 27, 6495-6506.	2.3	47
66	Structure and electronic state of molybdenum subcarbonyl species encaged in zeolite. The Journal of Physical Chemistry, 1991, 95, 3700-3705.	2.9	46
67	Synergy of Ru and Ir in the Electrohydrogenation of Toluene to Methylcyclohexane on a Ketjenblack-Supported Ru-Ir Alloy Cathode. ACS Catalysis, 2019, 9, 2448-2457.	11.2	46
68	The Polymer-Protected Pd–Pt Bimetallic Clusters Having Catalytic Activity for Selective Hydrogenation of Diene. Preparation and EXAFS Investigation on the Structure. Chemistry Letters, 1990, 19, 815-818.	1.3	45
69	Surface structure and catalysis for CO hydrogenation of the supported Ru species derived from the Ru3(CO)12 inorganic oxides. Journal of the Chemical Society, Faraday Transactions, 1990, 86, 2657.	1.7	45
70	Dynamical LEED analysis of Ni2P (0001)-1×1: Evidence for P-covered surface structure. Chemical Physics Letters, 2011, 513, 48-52.	2.6	45
71	Surface Structures and Catalytic Hydroformylation Activities of Rh Dimers Attached on Various Inorganic Oxide Supports. The Journal of Physical Chemistry, 1996, 100, 13636-13645.	2.9	44
72	Extended X-ray Absorption Fine Structure Studies on the Structure of the Poly(vinylpyrrolidone)-Stabilized Cu/Pd Nanoclusters Colloidally Dispersed in Solution. Journal of Physical Chemistry B, 2002, 106, 8587-8598.	2.6	44

#	Article	IF	CITATIONS
73	Controlling Length of Gold Nanowires with Large-Scale:  X-ray Absorption Spectroscopy Approaches to the Growth Process. Journal of Physical Chemistry C, 2007, 111, 18550-18557.	3.1	43
74	Photoexcited Hole Transfer to a MnOxCocatalyst on a SrTiO3Photoelectrode during Oxygen Evolution Studied by In Situ X-ray Absorption Spectroscopy. Journal of Physical Chemistry C, 2014, 118, 24302-24309.	3.1	42
75	Dynamics of Photoelectrons and Structural Changes of Tungsten Trioxide Observed by Femtosecond Transient XAFS. Angewandte Chemie - International Edition, 2016, 55, 1364-1367.	13.8	42
76	A New XAFS Beamline NW10A at the Photon Factory. AIP Conference Proceedings, 2007, , .	0.4	41
77	A structure model as the origin of catalytic properties of metal-doped MgO systems. Materials Chemistry and Physics, 1988, 18, 499-512.	4.0	39
78	The hydrogen exchange reaction of surface deuteroxyl groups on MgO with H2. Journal of the Chemical Society Faraday Transactions I, 1989, 85, 441.	1.0	39
79	Structure of one atomic layer titanium oxide on silica and its palladium-mediated restructuring. The Journal of Physical Chemistry, 1992, 96, 829-834.	2.9	39
80	Supported Gold Catalysts Derived from Gold Complexes and As-Precipitated Metal Hydroxides, Highly Active for Low-Temperature CO Oxidation. Chemistry Letters, 1996, 25, 755-756.	1.3	39
81	Preparations and catalytic properties of single, pair, and monolayer niobium catalysts. Catalysis Today, 1990, 8, 57-66.	4.4	38
82	Spatiotemporal concentration patterns associated with the catalytic oxidation of CO and Au covered Pt(110) surfaces. Journal of Chemical Physics, 1995, 102, 8175-8184.	3.0	38
83	In Situ Time-Resolved Energy-Dispersive XAFS Study on the Reduction Processes of Cu–ZSM-5 Catalysts. Bulletin of the Chemical Society of Japan, 2001, 74, 801-808.	3.2	38
84	Fabrication of Nanorattles with Passive Shell. Journal of Physical Chemistry B, 2006, 110, 19162-19167.	2.6	38
85	Analysis of EXAFS. Series on Synchrotron Radiation Techniques and Applications, 1996, , 33-58.	0.2	37
86	Three-Dimensional Structure Analyses of Cu Species Dispersed on TiO2(110) Surfaces Studied by Polarization-Dependent Total-Reflection Fluorescence X-ray Absorption Fine Structure (PTRF-XAFS). Journal of Physical Chemistry B, 2003, 107, 12917-12929.	2.6	37
87	Bimetallic copper-platinum particles supported in Y zeolite: structural characterization by EXAFS. The Journal of Physical Chemistry, 1991, 95, 5210-5215.	2.9	36
88	Ag L ₃ -Edge X-ray Absorption Near-Edge Structure of 4d ¹⁰ (Ag ⁺) Compounds: Origin of the Edge Peak and Its Chemical Relevance. Journal of Physical Chemistry A, 2010, 114, 4093-4098.	2.5	36
89	Structure of low coverage Ni atoms on the TiO2(110) surface – Polarization dependent total-reflection fluorescence EXAFS study. Chemical Physics Letters, 2006, 421, 27-30.	2.6	35
90	Fe K-Edge XANES and EXAFS of the X-Ray Absorption Spectra of FeCl3Aqueous Solutions. A Structural Study of the Solute, Iron(III) Chloro Complexes. Bulletin of the Chemical Society of Japan, 1985, 58, 1543-1550.	3.2	34

#	Article	IF	CITATIONS
91	Mixed valence oxide-dispersion-induced micropore filling of supercritical nitric oxide. The Journal of Physical Chemistry, 1992, 96, 10917-10922.	2.9	34
92	Spatio-temporal pattern formation during catalytic CO oxidation on a Pt(100) surface modified with submonolayers of Au. Surface Science, 1997, 374, 125-141.	1.9	34
93	Zeolite-encapsulated vanadium picolinate peroxo complexes active for catalytic hydrocarbon oxidations. Journal of Molecular Catalysis A, 1999, 137, 223-237.	4.8	34
94	Stepwise Synthesis and Structure Analysis of Mo Dimers in NaY Zeolite. Journal of Physical Chemistry B, 1999, 103, 1051-1058.	2.6	33
95	In Situ Time-Resolved Energy-Dispersive X-ray Absorption Fine Structure Study on the Decarbonylation Processes of Mo(CO)6 Entrapped in NaY and HY Zeolites. Journal of Physical Chemistry B, 2002, 106, 2415-2422.	2.6	33
96	Pdâ^'Câ^'Fe Nanoparticles Investigated by X-ray Absorption Spectroscopy as Electrocatalysts for Oxygen Reduction. Chemistry of Materials, 2009, 21, 4030-4036.	6.7	33
97	Promoting effects of Se on Rh/ZrO2 catalysis for ethene hydroformylation. Journal of Catalysis, 1991, 127, 631-644.	6.2	32
98	In situ observation of carrier transfer in the Mn-oxide/Nb:SrTiO3 photoelectrode by X-ray absorption spectroscopy. Chemical Communications, 2013, 49, 7848.	4.1	32
99	Extended x-ray absorption fine structure studies on the structure change of the alumina-attached [cobalt(II)]4 catalyst during carbon monoxide oxidation reaction. The Journal of Physical Chemistry, 1989, 93, 4213-4218.	2.9	31
100	Structural analysis of polymer-protected palladium/rhodium bimetallic clusters using EXAFS spectroscopy. The Journal of Physical Chemistry, 1993, 97, 10742-10749.	2.9	31
101	Modification of spatiotemporal pattern formation in an excitable medium by continuous variation of its intrinsic parameters: CO oxidation on Pt(110). Physical Review B, 1994, 50, 8043-8046.	3.2	31
102	Observation of Molecular Reaction Intermediate and Reaction Mechanism for NO Dissociation and No-H2 Reaction on Rh-Sn/SiO2 Catalysts. Journal of Catalysis, 1995, 157, 472-481.	6.2	31
103	PtL3-edge XANES studies about the hydrogen adsorption on small Pt particles. Journal of Synchrotron Radiation, 1999, 6, 439-441.	2.4	31
104	Development of anin situpolarization-dependent total-reflection fluorescence XAFS measurement system. Journal of Synchrotron Radiation, 2001, 8, 168-172.	2.4	31
105	Efficient Ru–Fe catalyzed selective hydrogenolysis of carboxylic acids to alcoholic chemicals. RSC Advances, 2014, 4, 29072-29082.	3.6	31
106	Self-regulated Ni cluster formation on the TiO2(110) terrace studied using scanning tunneling microscopy. Surface Science, 2006, 600, 117-121.	1.9	30
107	Preparation of atomically dispersed Cu species on a TiO2 (110) surface premodified with an organic compound. Chemical Physics Letters, 2007, 433, 345-349.	2.6	30
108	Scanning Tunneling Microscopy and Photoemission Electron Microscopy Studies on Single Crystal Ni ₂ P Surfaces. Journal of Nanoscience and Nanotechnology, 2009, 9, 195-201.	0.9	30

#	Article	lF	CITATIONS
109	Extended X-ray absorption fine structure and 129Xe nuclear magnetic resonance evidence for highly dispersed molybdenum clusters in zeolite Y. Journal of the Chemical Society, Faraday Transactions, 1990, 86, 1015.	1.7	29
110	Room-temperature-adsorption behavior of acetic anhydride on a TiO2(110) surface. Surface Science, 2007, 601, 1822-1830.	1.9	29
111	Quick X-ray Absorption Fine Structure Studies on the Activation Process of Ni ₂ P Supported on K-USY. Journal of Physical Chemistry C, 2011, 115, 7466-7471.	3.1	29
112	K-Edge X-ray Absorption Fine Structure Analysis of Pt/Au Core–Shell Electrocatalyst: Evidence for Short Pt–Pt Distance. Journal of Physical Chemistry C, 2014, 118, 8481-8490.	3.1	29
113	A study of FeN /C catalysts for the selective oxidation of unsaturated alcohols by molecular oxygen. Journal of Catalysis, 2018, 367, 16-26.	6.2	29
114	Synthesis and characterization of rhodium oxide nanoparticles in mesoporous MCM-41. Physical Chemistry Chemical Physics, 1999, 1, 2027-2032.	2.8	28
115	Title is missing!. Catalysis Letters, 1997, 46, 141-144.	2.6	27
116	Surface structures of Ni2P (0001)—scanning tunneling microscopy (STM) and low-energy electron diffraction (LEED) characterizations. Surface and Interface Analysis, 2006, 38, 1611-1614.	1.8	27
117	STM studies on the reconstruction of the Ni2P (101ì0) surface. Surface Science, 2010, 604, 1347-1352.	1.9	27
118	Temperature dependence of EXAFS spectra of supported small metal particles. Faraday Discussions, 1991, 92, 189.	3.2	26
119	Anisotropic structure analysis for Mo oxides on TiO2(110) single crystal surface by polarization-dependent total-reflection fluorescence EXAFS. Chemical Physics Letters, 1998, 288, 868-872.	2.6	26
120	Light-Induced Transformation of Molecular Materials into Devices. Advanced Materials, 2004, 16, 1786-1790.	21.0	26
121	THE SURFACE STRUCTURE AND CATALYTIC PROPERTIES OF ONE-ATOMIC LAYER AMORPHOUS NIOBIUM-OXIDE ATTACHED ON SiO2. Chemistry Letters, 1986, 15, 859-862.	1.3	25
122	Chemical environments around active sites and reaction mechanisms for deuterium–acrolein reaction over Ir/Nb2O5 in normal and SMSI states. Journal of the Chemical Society Faraday Transactions I, 1989, 85, 2021.	1.0	25
123	Anisotropic structure analysis for cobalt oxides on ?-Al2O3(0001) by polarized total-reflection fluorescence extended X-ray absorption fine structure. Catalysis Letters, 1992, 15, 247-254.	2.6	25
124	Characterization of rhodium oxide nanoparticles in MCM-41 and their catalytic performances for NO–CO reactions in excess O2. Applied Catalysis A: General, 2002, 228, 305-314.	4.3	25
125	Effect of application time of colloidal platinum nanoparticles on the microtensile bond strength to dentin. Dental Materials Journal, 2010, 29, 682-689.	1.8	25
126	Carbon incorporated FeN/C electrocatalyst for oxygen reduction enhancement in direct methanol fuel cells: X-ray absorption approach to local structures. Electrochimica Acta, 2011, 56, 8734-8738.	5.2	25

#	Article	IF	CITATIONS
127	An XAFS study on the specific microstructure of active species in iron titanate catalyst for NH3-SCR of NOx. Catalysis Today, 2013, 201, 131-138.	4.4	25
128	Density Function Theoretical Investigation on the Ni3PP Structure and the Hydrogen Adsorption Property of the Ni2P(0001) Surface. Chemistry Letters, 2013, 42, 1481-1483.	1.3	25
129	Deprotonation of a dinuclear copper complex of 3,5-diamino-1,2,4-triazole for high oxygen reduction activity. Physical Chemistry Chemical Physics, 2015, 17, 8638-8641.	2.8	25
130	Trace mono-atomically dispersed rhodium on zeolite-supported cobalt catalyst for the efficient methane oxidation. Communications Chemistry, 2018, 1, .	4.5	25
131	Mechanistic study of the selective hydrogenation of carboxylic acid derivatives over supported rhenium catalysts. Catalysis Science and Technology, 2019, 9, 5413-5424.	4.1	25
132	Transfer hydrogenolysis of aromatic ethers promoted by the bimetallic Pd/Co catalyst. Catalysis Today, 2020, 357, 511-517.	4.4	25
133	Exafs study of FeCl3-doped polyacetylene. Solid State Communications, 1983, 46, 235-238.	1.9	24
134	Characterization of Pt/SbOxCatalysts Active for Selective Oxidation of Isobutane by Means of XRD, TEM, and XAFS. Journal of Catalysis, 1997, 171, 457-466.	6.2	24
135	Vanadium(IV) complexes with picolinic acids in NaY zeolite cages Synthesis, characterization and catalytic behaviour. Journal of the Chemical Society, Faraday Transactions, 1998, 94, 809-816.	1.7	24
136	In situ XAFS analysis of Pd–Pt catalysts during hydrotreatment of model oil. Catalysis Today, 2006, 111, 199-204.	4.4	24
137	Adsorbed structure of copper and calcium dipivaloylmethanates on SiO2. Surface Science, 1992, 278, 175-182.	1.9	23
138	Synthesis and characterization of vanadium (IV) complexes in NaY zeolite supercages. Microporous and Mesoporous Materials, 1998, 21, 571-579.	4.4	23
139	A local structure of low coverage Ni species on the α-Al2O3 (0001) surface – a polarization dependent EXAFS study. Chemical Physics Letters, 2004, 384, 134-138.	2.6	23
140	X-ray Absorption Fine Structure (XAFS) Analysis of Titanium-implanted Soft Tissue. Dental Materials Journal, 2007, 26, 268-273.	1.8	23
141	Structural analysis of strontium in human teeth treated with surface pre-reacted glass-ionomer filler eluate by using extended X-ray absorption fine structure analysis. Dental Materials Journal, 2017, 36, 214-221.	1.8	23
142	Selective isopentane formation from CH3OH on a new one-atomic layer ZrO2/ZSM-5 hybrid catalyst. Catalysis Letters, 1988, 1, 395-403.	2.6	22
143	Rhodium-niobia interaction in niobia-promoted Rh/SiO2 catalysts: formation of RhNbO4 on SiO2. Catalysis Today, 1990, 8, 85-97.	4.4	22
144	Monolayer structures of niobic acids supported on silica and their catalytic activities for esterification of acetic acid with ethanol. The Journal of Physical Chemistry, 1991, 95, 9999-10004.	2.9	22

#	Article	IF	CITATIONS
145	Structures and catalytic activity of Pt\$z.sbnd;Mo bimetallic ensembles derived from a new planar 6PtMo6O2498\$minus; heteropolyanion supported on Al2O3 and SiO2I. Characterization of the supported 6PtMo69 catalysts. Journal of Catalysis, 1992, 135, 367-385.	6.2	22
146	Catalysis on mesoscopic composite surfaces: Influence of palladium boundaries on pattern formation during CO oxidation on Pt(1 1 0). Physica D: Nonlinear Phenomena, 1998, 123, 493-501.	2.8	22
147	X-ray photoemission electron microscopy (XPEEM) as a new promising tool for the real-time chemical imaging of active surfaces. Journal of Molecular Catalysis A, 1999, 141, 129-137.	4.8	22
148	Surface catalytic reactions assisted by gas phase molecules: activation of reaction intermediates. Journal of Molecular Catalysis A, 2000, 163, 67-77.	4.8	22
149	Characterization of Rh Particles and Li-Promoted Rh Particles in Y Zeolite during CO2 Hydrogenation—A New Mechanism for Catalysis Controlled by the Dynamic Structure of Rh Particles and the Li Additive Effect. Journal of Catalysis, 2000, 194, 91-104.	6.2	22
150	Origin of Self-Regulated Cluster Growth on the TiO ₂ (110) Surface Studied Using Polarization-Dependent Total Reflection Fluorescence XAFS. Journal of Physical Chemistry C, 2008, 112, 4667-4675.	3.1	22
151	Molecular Catalysts Confined on and Within Molecular Layers Formed on a Si(111) Surface with Direct Si–C Bonds. Advanced Materials, 2012, 24, 268-272.	21.0	22
152	Preparation and structure of a single Au atom on the TiO2(110) surface: control of the Au–metal oxide surface interaction. Faraday Discussions, 2013, 162, 165.	3.2	22
153	In Situ Picosecond XAFS Study of an Excited State of Tungsten Oxide. Chemistry Letters, 2014, 43, 977-979.	1.3	22
154	<i>Operando</i> Observations of a Manganese Oxide Electrocatalyst for Water Oxidation Using Hard/Tender/Soft X-ray Absorption Spectroscopy. Journal of Physical Chemistry C, 2020, 124, 23611-23618.	3.1	22
155	Role of Oxygen Vacancy in the Photocarrier Dynamics of WO ₃ Photocatalysts: The Case of Recombination Centers. Journal of Physical Chemistry C, 2022, 126, 9257-9263.	3.1	22
156	Structure and Catalysis of a SiO2-Supported Gold-Platinum Cluster [(PPh3)Pt(PPh3Au)6](NO3)2. Chemistry Letters, 1996, 25, 129-130.	1.3	21
157	Energy-dispersive XAFS study on the decarbonylation process of Mo(CO)6 in NaY zeolite. Catalysis Letters, 2001, 71, 203-208.	2.6	21
158	Design of a high-temperature and high-pressure liquid flow cell for x-ray absorption fine structure measurements under catalytic reaction conditions. Review of Scientific Instruments, 2008, 79, 014101.	1.3	21
159	Structural Relationship between CoO ₆ Cluster and Phosphate Species in a Cobalt–Phosphate Water Oxidation Catalyst Investigated by Co and P K-edge XAFS. Chemistry Letters, 2016, 45, 277-279.	1.3	21
160	Structure determination of the rutile-TiO ₂ (110)-(1 × 2) surface using total-reflection high-energy positron diffraction (TRHEPD). Physical Chemistry Chemical Physics, 2016, 18, 7085-7092.	2.8	21
161	SPECTROSCOPIC STUDIES ON THE SURFACE STRUCTURES OF RUTHENIUM CATALYSTS DERIVED FROM Ru3(CO)12/Î ³ -Al2O3OR SiO2. Chemistry Letters, 1985, 14, 511-514.	1.3	20
162	Metal-assisted CO insertion reaction on a new surface rhodium dimer catalyst observed by an in situ EXAFS technique. Journal of the American Chemical Society, 1990, 112, 3242-3244.	13.7	20

#	Article	IF	CITATIONS
163	Asymmetric Structure Determination of Copper Oxide on α-Quartz(0001) Surface by Polarized Total-Reflection Fluorescence Extended X-Ray Absorption Fine Structure Spectroscopy. Chemistry Letters, 1992, 21, 1037-1040.	1.3	20
164	Nanosized rhodium oxide particles in the MCM-41 mesoporous molecular sieve. Chemical Communications, 1998, , 1425-1426.	4.1	20
165	Local structure of Pt and Pd ions in Ce1â^'xTixO2: X-ray diffraction, x-ray photoelectron spectroscopy, and extended x-ray absorption fine structure. Journal of Chemical Physics, 2008, 128, 124711.	3.0	20
166	Temporal Analysis of Products (TAP) Study of the Adsorption of CO, O2, and CO2on a Au/Ti(OH)4*Catalyst. Bulletin of the Chemical Society of Japan, 2001, 74, 255-265.	3.2	19
167	Methanol steam reforming behavior of sol-gel synthesized nanodimensional CuxFe1-xAl2O4 hercynites. Applied Catalysis A: General, 2019, 570, 73-83.	4.3	19
168	EXAFS Spectroscopy of Some Iron(III) Compounds by Use of Dispersive-type In-laboratory X-Ray Spectrometer. Bulletin of the Chemical Society of Japan, 1982, 55, 3911-3914.	3.2	18
169	Asymmetric structure analysis of active surface-sites by in situ polarized total-reflection fluorescence EXAFS. Catalysis Letters, 1993, 20, 117-124.	2.6	18
170	A new characterization method for adsorbed hydrogen on supported Pt particles. Studies in Surface Science and Catalysis, 1996, 101, 911-919.	1.5	18
171	Multiple Scattering Approach to PtL3-edge X-Ray Absorption near Edge Structure Spectra of Small Pt Clusters with Hydrogen Adsorption. Japanese Journal of Applied Physics, 1997, 36, 6504-6510.	1.5	18
172	The interaction of Pt and SbOx in the selective oxidation of isobutylene to methacrolein. Applied Catalysis A: General, 1997, 165, 183-197.	4.3	18
173	Characterization and catalysis of a SiO2-supported [Au6Pt] cluster [(AuPPh3)6Pt(PPh3)]2+/SiO2. Journal of Molecular Catalysis A, 1997, 122, 147-157.	4.8	18
174	Characterization and selective oxidation catalysis of modified Pt particles on SbOx. Applied Catalysis A: General, 2000, 191, 131-140.	4.3	18
175	The First Observation of an Atomic Scale Noncontact AFM Image of MoO3(010). Chemistry Letters, 2003, 32, 1098-1099.	1.3	18
176	Polarization-Dependent Total-Reflection Fluorescence X-ray Absorption Fine Structure for 3D Structural Determination and Surface Fine Tuning. Topics in Catalysis, 2013, 56, 1477-1487.	2.8	18
177	In situ back-side illumination fluorescence XAFS (BI-FXAFS) studies on platinum nanoparticles deposited on a HOPG surface as a model fuel cell: a new approach to the Pt-HOPG electrolyte interface. Physical Chemistry Chemical Physics, 2014, 16, 13748-13754.	2.8	18
178	Pt-Promoted Cu/SBA-15 Catalysts with Excellent Performance for Chemoselective Hydrogenation of Dimethyl Oxalate to Ethylene Glycol. Topics in Catalysis, 2014, 57, 1015-1025.	2.8	18
179	Sol–gel chemistry mediated Zn/Al-based complex dispersant for SWCNT in water without foam formation. Carbon, 2015, 94, 518-523.	10.3	18
180	An Investigation of Ni2P Single Crystal Surfaces: Structure, Electronic State and Reactivity. Topics in Catalysis, 2015, 58, 194-200.	2.8	18

#	Article	IF	CITATIONS
181	Capturing local structure modulations of photoexcited BiVO ₄ by ultrafast transient XAFS. Chemical Communications, 2017, 53, 7314-7317.	4.1	18
182	Characterization of GeO2Sub-monolayers on SiO2Prepared by Chemical Vapor Deposition of Ge(OMe)4by EXAFS, FT-IR, and XRD. Langmuir, 1998, 14, 3607-3613.	3.5	17
183	Pd L3-Edge XANES Spectra of Supported Pd Particles Induced by the Adsorption and the Absorption of Hydrogen. Bulletin of the Chemical Society of Japan, 1999, 72, 673-681.	3.2	17
184	The challenge of constructing an international XAFSÂdatabase. Journal of Synchrotron Radiation, 2018, 25, 967-971.	2.4	17
185	Polarization-dependent total reflection fluorescence extended X-ray absorption fine structure and its application to supported catalysis. Catalysis, 2012, , 281-322.	1.0	17
186	New Reversible Enhancement/Depression Phenomenon on Catalysis of Platinum Supported on One-Atomic Layer Niobium Oxide for Ethene Hydrogenation. Chemistry Letters, 1988, 17, 633-636.	1.3	16
187	Zeolite supported PtRh catalysts for CO oxidation and NO reduction: Evidence for bimetallic particles formation and synergism effect. Catalysis Letters, 1991, 11, 33-40.	2.6	16
188	In situ polarized total-reflection fluorescence X-ray absorption near-edge structure spectroscopy for the analysis of oriented structure of vanadium oxides on ZrO2(100). Catalysis Letters, 1994, 26, 229-234.	2.6	16
189	Development of a chamber for in situ polarized totalâ€reflection fluorescence xâ€ray absorption fine structure spectroscopy. Review of Scientific Instruments, 1995, 66, 5493-5498.	1.3	16
190	Surface structure change of a [Pt4(Âμ-CH3COO)8]/SiO2catalyst active for the decomposition of formic acid. Journal of the Chemical Society, Faraday Transactions, 1995, 91, 4161-4170.	1.7	16
191	Catalytic Behavior of Pt/SbOxfor Selective Oxidation of i-C4H10and i-C4H8in Stationary and Nonstationary Conditions. Journal of Catalysis, 1997, 171, 184-190.	6.2	16
192	Title is missing!. Topics in Catalysis, 2000, 10, 209-219.	2.8	16
193	A Scanning Tunneling Microscopy Observation of (\$sqrt{3}imessqrt{3}\$) R30° Reconstructed Ni2P(0001). Japanese Journal of Applied Physics, 2008, 47, 6088-6091.	1.5	16
194	First Direct Visualization of Spillover Species Emitted from Pt Nanoparticles. Langmuir, 2010, 26, 16392-16396.	3.5	16
195	A new TiO2-attached rhodium metal catalyst. Catalyst characterization and non-SMSI behaviour. Journal of the Chemical Society Faraday Transactions I, 1988, 84, 1329.	1.0	15
196	Promoting effects of Se on Rh/SiO2 catalysis for ethene hydroformylation. Journal of Catalysis, 1991, 132, 566-570.	6.2	15
197	Reversible structure transformation of zirconium dioxide on palladium black. The Journal of Physical Chemistry, 1992, 96, 7386-7389.	2.9	15
198	A "Cluster-in-Cluster―Structure of the SiO ₂ -Supported PtPd Clusters. Japanese Journal of Applied Physics, 1993, 32, 448.	1.5	15

#	Article	IF	CITATIONS
199	A new aspect of catalysis at designed surfaces: the role of gas phase molecules in surface catalytic reactions. Journal of Molecular Catalysis A, 1999, 146, 65-76.	4.8	15
200	In Situ X-ray Absorption Fine Structure Studies on the Structure of Nickel Phosphide Catalyst Supported on K-USY. Chemistry Letters, 2003, 32, 956-957.	1.3	15
201	Operando QEXAFS studies of Ni ₂ P during thiophene hydrodesulfurization: direct observation of Ni—S bond formation under reaction conditions. Journal of Synchrotron Radiation, 2012, 19, 205-209.	2.4	15
202	Incorporation of Multinuclear Copper Active Sites into Nitrogen-Doped Graphene for Electrochemical Oxygen Reduction. ACS Applied Energy Materials, 2018, 1, 2358-2364.	5.1	15
203	Photoinduced anisotropic distortion as the electron trapping site of tungsten trioxide by ultrafast W L ₁ -edge X-ray absorption spectroscopy with full potential multiple scattering calculations. Physical Chemistry Chemical Physics, 2020, 22, 2615-2621.	2.8	15
204	EXAFS Studies of the Behavior of Rh6(CO)16Supported on Î ³ -Al2O3Surface. Bulletin of the Chemical Society of Japan, 1986, 59, 647-648.	3.2	14
205	Zirconium oxide supported on Pd(100): Characterization by scanning tunneling microscopy and tunneling spectroscopy. Catalysis Letters, 1992, 15, 317-327.	2.6	14
206	Promoting effects of Sn on NO dissociation and NO reduction with H2on Rh–Sn/SiO2catalysts. Journal of the Chemical Society Chemical Communications, 1993, .	2.0	14
207	Structural Analysis of Chelate Resin-Iron Complex by Using Extended X-ray Absorption Fine Structure Spectroscopy. The Journal of Physical Chemistry, 1994, 98, 7967-7975.	2.9	14
208	Structure and catalytic performance of Mo dimer oxy-carbide species in NaY supercages. Applied Catalysis A: General, 2000, 194-195, 365-374.	4.3	14
209	Preparation, Characterization, and Catalytic Performance of Bismuthâ `Aluminum Binary-Oxide Layers and Clusters on an Al2O3Surface. Journal of Physical Chemistry B, 2000, 104, 12263-12268.	2.6	14
210	Electronic structure of the surface: Angle-resolved photoemission study. Solid State Communications, 2010, 150, 1120-1123.	1.9	14
211	Fine tuning and orientation control of surface Cu complexes on TiO2(110) premodified with mercapto compounds: the effect of different mercapto group positions. Physical Chemistry Chemical Physics, 2013, 15, 14080.	2.8	14
212	EXAFS Studies of Pd Nanoparticles: Direct Evidence for Unusual Pd–Pd Bond Elongation. Chemistry Letters, 2015, 44, 803-805.	1.3	14
213	Effective surface termination with Au on PtCo@Pt core-shell nanoparticle: Microstructural investigations and oxygen reduction reaction properties. Journal of Electroanalytical Chemistry, 2019, 842, 1-7.	3.8	14
214	Dopant Structure in FeCl3-doped Polyacetylene Studied by X-Ray Absorption Spectroscopy and X-Ray Photoelectron Spectroscopy. Bulletin of the Chemical Society of Japan, 1985, 58, 2113-2120.	3.2	13
215	Multiple Scattering Approach to Pd L3-Edge X-Ray Absorption near Edge Structure Spectra for Small Pd Clusters with Hydrogen Adsorption and Absorption. Japanese Journal of Applied Physics, 1998, 37, 4134-4139.	1.5	13
216	Observation of Energy-Filtered Image for X-Ray Photoemission Electron Microscopy (EXPEEM) Using a Retarding Wien-Filter Energy Analyzer. Chemistry Letters, 2002, 31, 842-843.	1.3	13

#	Article	IF	CITATIONS
217	Development of imaging energy analyzer using multipole Wien filter. Applied Surface Science, 2005, 241, 131-134.	6.1	13
218	Atomically dispersed Cu species on a TiO2(110) surface precovered with acetic anhydride. Chemical Physics Letters, 2009, 470, 99-102.	2.6	13
219	Operando Observation of Ni2P Structural Changes during Catalytic Reaction: Effect of H2S Pretreatment. Chemistry Letters, 2012, 41, 1238-1240.	1.3	13
220	Investigation of the Cleanliness of Transferred Graphene: The First Step toward Its Application as a Window Material for Electron Microscopy and Spectroscopy. Bulletin of the Chemical Society of Japan, 2015, 88, 1029-1035.	3.2	13
221	Various Active Metal Species Incorporated within Molecular Layers on Si(111) Electrodes for Hydrogen Evolution and CO ₂ Reduction Reactions. Journal of Physical Chemistry C, 2016, 120, 16200-16210.	3.1	13
222	Metamorphosis-like Transformation during Activation of In/SiO ₂ Catalyst for Non-oxidative Coupling of Methane: <i>In Situ</i> X-ray Absorption Fine Structure Analysis. Chemistry Letters, 2019, 48, 1145-1147.	1.3	13
223	The structures and synergistic catalyses of FeRu/Al2O3 catalysts derived from FexRu3–x(CO)12(x= 0, 1,) Tj ETC Society Faraday Transactions I, 1988, 84, 2445.	2q1 1 0.78 1.0	4314 rgBT / 12
224	Temperature dependence of EXAFS spectra of rhodium and palladium catalysts in the strong metal-support interaction state. The Journal of Physical Chemistry, 1989, 93, 8323-8327.	2.9	12
225	The structure analysis of MoOx/TiO2(110) by polarization-dependent total-reflection fluorescence X-ray absorption fine structure. Catalysis Today, 1998, 44, 309-314.	4.4	12
226	Development of an X-ray photoemission electron microscopy system with multi-probes, and its application to surface imaging at static and dynamic states. Journal of Microscopy, 2000, 200, 240-250.	1.8	12
227	Three-dimensional analysis of the local structure of Cu on TiO2(110) byin situpolarization-dependent total-reflection fluorescence XAFS. Journal of Synchrotron Radiation, 2001, 8, 508-510.	2.4	12
228	UV-vis-Induced Vitrification of a Molecular Crystal. Advanced Functional Materials, 2007, 17, 1663-1670.	14.9	12
229	Adsorption structure of acetic anhydride on a TiO2(110) surface observed by scanning tunneling microscopy. Surface Science, 2009, 603, 552-557.	1.9	12
230	Carbon Monoxide Hydrogenation on SiO2â^', Al2O3â^', or TiO2-Attached Nb-Monomer Catalysts. Chemistry Letters, 1987, 16, 573-576.	1.3	11
231	Synthesis, X-Ray Analysis, EXAFS, and XANES of [Ni(SCH2CH2S)2]2â^'. An Evidence for the Mononuclear Square Planar {Ni(II)Sâ^'4} Geometry in Nickel/Alkane Thiolate System. Chemistry Letters, 1990, 19, 101-104.	1.3	11
232	Preparation and catalytic properties of a new SiO2-attached Nb-dimer catalyst: regulation of acidity–basicity by the number of metal atoms in surface active sites. Journal of the Chemical Society Chemical Communications, 1991, , 112-113.	2.0	11
233	In-situEXAFS Observation of the Molecular Reaction Intermediate for NO–H2Reaction on Highly Active Rh–Sn/SiO2Catalysts. Chemistry Letters, 1994, 23, 235-238.	1.3	11
234	In-situ asymmetric structure analysis of Pt clusters on α-Al2O3(0 0 0 1) in H2 reduction and NO adsorption. Physica B: Condensed Matter, 1995, 208-209, 637-640.	2.7	11

#	Article	IF	CITATIONS
235	Dispersive XAFS Study on Cu and Mo Species in Zeolites During the Catalyst Preparation. Topics in Catalysis, 2002, 18, 53-58.	2.8	11
236	Title is missing!. Catalysis Surveys From Asia, 2003, 7, 177-182.	2.6	11
237	Observation of Element-Specific Energy-Filtered X-Ray Photoemission Electron Microscopy Images of Au on Ta Using a Wien Filter Type Energy Analyzer. Japanese Journal of Applied Physics, 2004, 43, 7682-7688.	1.5	11
238	Analysis of Titanium Dental Implants Surrounding Soft Tissue Using X-ray Absorption Fine Structure (XAFS) Analysis. Chemistry Letters, 2005, 34, 776-777.	1.3	11
239	Aberration-corrected multipole Wien filter for energy-filtered x-ray photoemission electron microscopy. Review of Scientific Instruments, 2007, 78, 063710.	1.3	11
240	Au Clusters on TiO ₂ (110) (1 × 1) and (1 × 2) Surfaces Examined by Polarization-Dependent Total Reflection Fluorescence XAFS. Journal of Physical Chemistry C, 2013, 117, 252-257.	3.1	11
241	Improvement of a Real Gas-Sensor for the Origin of Methane Selectivity Degradation by µ-XAFS Investigation. Nano-Micro Letters, 2015, 7, 255-260.	27.0	11
242	Reaction Stoichiometry and Mechanism of Pt Deposition via Surface Limited Redox Replacement of Copper UPD Layer on Au(111). Journal of Physical Chemistry C, 2018, 122, 16664-16673.	3.1	11
243	Disposition of Iridium on Ruthenium Nanoparticle Supported on Ketjenblack: Enhancement in Electrocatalytic Activity toward the Electrohydrogenation of Toluene to Methylcyclohexane. ACS Omega, 2020, 5, 1221-1228.	3.5	11
244	Expansion of nanotechnology for dentistry: effect of colloidal platinum nanoparticles on dentin adhesion mediated by 4-META/MMA-TBB. Journal of Adhesive Dentistry, 2011, 13, 411-6.	0.5	11
245	STRUCTURAL STUDY OF POLY(CARBON DISELENIDE). Chemistry Letters, 1985, 14, 1-4.	1.3	10
246	Measurements of the extended X-ray absorption fine structure (EXAFS) spectra at the K edges of cerium, praseodymium and samarium compounds with synchrotron radiation. Journal of Physics C: Solid State Physics, 1987, 20, 5027-5035.	1.5	10
247	Structures and dynamic behavior of catalyst model surfaces characterized by modern physical techniques. Research on Chemical Intermediates, 1998, 24, 151-168.	2.7	10
248	Polarization-dependent EXAFS studies on the structures of Mo oxides dispersed on single crystals. Journal of Electron Spectroscopy and Related Phenomena, 2001, 119, 185-192.	1.7	10
249	Polarization-Dependent EXAFS Measurements of an α-Molybdenum Trioxide Single Crystal. Topics in Catalysis, 2002, 18, 125-127.	2.8	10
250	A Possibility of XANAM (X-ray Aided Non-contact Atomic Force Microscopy). Chemistry Letters, 2004, 33, 636-637.	1.3	10
251	EXAFS Studies about the Sorption of Cadmium Ions on Montmorillonite. Chemistry Letters, 2006, 35, 224-225.	1.3	10
252	Chemical States of Ag in Ag(DMe-DCNQI)2 Photoproducts and a Proposal for Its Photoinduced Conductivity Change Mechanism. Chemistry Letters, 2007, 36, 1008-1009.	1.3	10

#	Article	IF	CITATIONS
253	Combined in situ analysis of Ni ₂ P/MCM-41 under hydrodesulfurization conditions – Simultaneous observation of QXAFS and FTIR –. Journal of Physics: Conference Series, 2009, 190, 012158.	0.4	10
254	Atomic aspects of surface chemical reactions. Catalysis Today, 2010, 157, 2-7.	4.4	10
255	Angle resolved total reflection fluorescence XAFS and its application to Au clusters on TiO2(110) (1 *) Tj ETQq1 1	0.784314 1.1	4 rgBT /Ove 10
256	A New Indicator for Single Metal Dispersion on a TiO ₂ (110) Surface Premodified with a Mercapto Compound. Journal of Physical Chemistry C, 2016, 120, 15785-15791.	3.1	10
257	Polarization-dependent Total Reflection Fluorescence X-ray Absorption Fine Structure (PTRF-XAFS) Studies on the Structure of a Pt Monolayer on Au(111) Prepared by the Surface-limited Redox Replacement Reaction. Chemistry Letters, 2017, 46, 1250-1253.	1.3	10
258	XFELs: cutting edge X-ray light for chemical and material sciences. Physical Chemistry Chemical Physics, 2020, 22, 2612-2614.	2.8	10
259	Surface Structure of Low Coverage Chlorine Adsorbed on a Nickel Stepped Surface. Japanese Journal of Applied Physics, 1993, 32, 368.	1.5	10
260	Spectroscopic evidence for a surface Nb carbene in a new SiO2-attached Nb catalyst active for propene metathesis. Journal of Molecular Catalysis, 1989, 55, 159-169.	1.2	9
261	A new structure and hydrogenation activity of Fe3(CO)12 supported on SiRx(R:CH3, C6H5)-modified SiO2 surfaces. Journal of Molecular Catalysis, 1992, 74, 345-351.	1.2	9
262	Structural Analysis of Polymer-Protected Pd/Rh Bimetallic Clusters by Using EXAFS Spectroscopy. Japanese Journal of Applied Physics, 1993, 32, 451.	1.5	9
263	PTRF X-ray absorption fine structure as a new technique for catalyst characterization. Journal of Molecular Catalysis A, 1996, 107, 55-65.	4.8	9
264	Surface structure analysis of dispersed metal sites on single crystal metal oxides by means of polarization-dependent total-reflection fluorescent EXAFS. Applied Surface Science, 1996, 100-101, 143-146.	6.1	9
265	Structural Transformation and Low-Pressure Catalysis for Ethyl Acetate Hydrogenation of Rh/One-Atomic-Layer GeO2/SiO2. Journal of Physical Chemistry B, 1997, 101, 9984-9990.	2.6	9
266	Time-resolved energy-dispersive XAFS study on the reduction process of Cu-ZSM-5 catalysts. Journal of Synchrotron Radiation, 2001, 8, 654-656.	2.4	9
267	Surface Reactions on MoO3Induced by Tunable Pulse Infrared Free Electron Laser. Chemistry Letters, 2004, 33, 558-559.	1.3	9
268	What is the Interaction between Atomically Dispersed Ni and Oxide Surfaces?. Materials Transactions, 2009, 50, 509-515.	1.2	9
269	Microscopic Structure of Naked Au Nanoparticles Synthesized in Typical Ionic Liquids by Sputter Deposition. Journal of Physical Chemistry C, 2014, 118, 27973-27980.	3.1	9
270	Model building analysis – a novel method for statistical evaluation of Pt L ₃ -edge EXAFS data to unravel the structure of Pt-alloy nanoparticles for the oxygen reduction reaction on highly oriented pyrolytic graphite. Physical Chemistry Chemical Physics, 2020, 22, 18815-18823.	2.8	9

#	Article	IF	CITATIONS
271	Structures and synergistic catalyses of FeRu/Al2O3 catalysts derived from FexRu3–x(CO)12(x= 0, 1, 2, 3). Part 2.—Structures and catalyses of FeRu catalysts reduced with H2. Journal of the Chemical Society Faraday Transactions I, 1988, 84, 2457.	1.0	8
272	Local reaction environments and their properties for ethene deuterogenation on the surfaces of SMSI catalysts. Journal of the Chemical Society Faraday Transactions I, 1988, 84, 4337.	1.0	8
273	Direct observation of unusual CO insertion on a new SiO2-attached Rh dimer catalyst by FTIR. Journal of the Chemical Society Chemical Communications, 1990, , 253.	2.0	8
274	Formation of coordinatively unsaturated H2FeOs3(CO)12 in solid matrixes at 77 K by irradiation of H2FeOs3(CO)13: a model for the photoreaction postulated to form H2FeOs3(CO)12 on the surface of silica. The Journal of Physical Chemistry, 1992, 96, 9565-9568.	2.9	8
275	Photochemical reaction of H2FeOs3(CO)13 adsorbed on the surface of silica. The Journal of Physical Chemistry, 1992, 96, 6367-6371.	2.9	8
276	Application of a CdTe Solid-State Detector to Polarization-Dependent Total-Reflection Fluorescence XAFS Measurements. Journal of Synchrotron Radiation, 1996, 3, 160-162.	2.4	8
277	X-ray Absorption Fine Structure Studies on the Local Structures of Ni Impurities in a Carbon Nanotube. Chemistry Letters, 2005, 34, 382-383.	1.3	8
278	Selenium Distribution in Human Soft Tissue Determined by Using X-ray Scanning Analytical Microscope and X-ray Absorption Fine Structure Analysis. Chemistry Letters, 2006, 35, 66-67.	1.3	8
279	Origin of Photochemical Modification of the Resistivity of Ag(DMe-DCNQI) ₂ Studied by X-ray Absorption Fine Structure. Journal of Physical Chemistry C, 2009, 113, 20476-20480.	3.1	8
280	Preparation of well-crystallized Pd20Te7 alloy nanoparticulate catalysts with uniform structure and composition in liquid-phase. Applied Catalysis A: General, 2011, 392, 80-85.	4.3	8
281	Smooth epitaxial copper film on sapphire surface suitable for high quality graphene growth. Thin Solid Films, 2018, 646, 12-16.	1.8	8
282	Thorough Search Analysis of Extended X-ray Absorption Fine Structure Data for Complex Molecules and Nanomaterials Applications. E-Journal of Surface Science and Nanotechnology, 2020, 18, 249-261.	0.4	8
283	Anisotropic Arrangement of Mo Species Highly Dispersed on TiO ₂ (110) Surface Demonstrated by Polarization Dependent Total Reflection Fluorescence EXAFS. Japanese Journal of Applied Physics, 1999, 38, 40.	1.5	8
284	New Inorganic Oxide-attached Nb Catalysts Active for Propene Metathesis. Chemistry Letters, 1986, 15, 1457-1460.	1.3	7
285	Characterization of bimetallic surface structures of highly active Rh-Sn/SiO2 catalysts for NO-H2 reaction by EXAFS. Catalysis Letters, 1993, 20, 15-22.	2.6	7
286	Structural properties of [(AuPH3)6Pt(H2)(PH3)]2+: theoretical study of dihydrogen activation. Chemical Physics Letters, 1998, 286, 163-170.	2.6	7
287	Characterization of CO- and H2-Adsorbed Au6Pt-Phosphine Clusters Supported on SiO2by EXAFS, TPD, and FTIR. Bulletin of the Chemical Society of Japan, 1999, 72, 2643-2653.	3.2	7
288	Anisotropic ordering of Mo species deposited on TiO2(1 1 0) characterized by polarization-dependent total reflection fluorescence EXAFS (PTRF-EXAFS). Catalysis Today, 2001, 66, 97-103.	4.4	7

#	Article	IF	CITATIONS
289	Preparation and Characterization of a Microfabricated Oxide-on-Oxide Catalyst of α-Sb2O4/VSbO4. Bulletin of the Chemical Society of Japan, 2005, 78, 435-442.	3.2	7
290	Development of in-lab energy-filtered X-ray photoemission electron microscope using air-core-coil-type multipole Wien filter. Surface Science, 2007, 601, 4742-4747.	1.9	7
291	Energy-filtered X-ray photoemission electron microscopy and its applications to surface and organic materials. Solid-State Electronics, 2007, 51, 1360-1366.	1.4	7
292	Infrared-Induced Reaction on MoO3 Using a Tunable Infrared Free Electron Laser. Bulletin of the Chemical Society of Japan, 2008, 81, 836-842.	3.2	7
293	XAFS Analysis of the Bronchoalveolar Lavage Fluid of a Tungsten Carbide Pneumoconiosis Patient. Chemistry Letters, 2010, 39, 852-853.	1.3	7
294	International Workshop on Improving Data Quality and Quantity for XAFS Experiments (Q2XAFS 2011). Journal of Synchrotron Radiation, 2012, 19, 849-850.	2.4	7
295	Phosphorous Diffusion Through Ni ₂ P—Low Energy Diffusion Path and Its Unique Local Structure. Journal of Physical Chemistry C, 2018, 122, 6318-6322.	3.1	7
296	Active Phase Structure of the SiO ₂ -supported Nickel Phosphide Catalysts for Non-oxidative Coupling of Methane (NOCM) Reactions. E-Journal of Surface Science and Nanotechnology, 2020, 18, 24-27.	0.4	7
297	TEMPERATURE DEPENDENCE OF THE Pt L ₃ -EDGE EXAFS OF PLATINUM CLUSTERS SUPPORTED ON NaY-ZEOLITE. Journal De Physique Colloque, 1986, 47, C8-273-C8-276.	0.2	7
298	Atomic Structure and Catalytic Activity of W-Modified Ni ₂ P Surface Alloy by Photoelectron Diffraction and Spectroscopy. E-Journal of Surface Science and Nanotechnology, 2014, 12, 53-56.	0.4	7
299	Promoting effects of Se on the activity and selectivity of Rh–ZrO2catalyst for ethene hydroformylation. Journal of the Chemical Society Chemical Communications, 1988, , 1327-1328.	2.0	6
300	Bis(2-pyridinecarboxylato)vanadium(IV) in NaY Zeolite Cages: Synthesis and Spectroscopic Properties. Chemistry Letters, 1997, 26, 313-314.	1.3	6
301	Nanoparticles of RhOx in the MCM-41: a novel catalyst for NO-CO reaction in excess O 2. Scripta Materialia, 2001, 44, 1695-1698.	5.2	6
302	Multiple scattering approach to the Pt L2-edge XANES of CO adsorption on small Pt particles. Chemical Physics Letters, 2002, 357, 365-370.	2.6	6
303	Theoretical Debye–Waller factors of α-MoO3estimated by an equation-of-motion method. Journal of Synchrotron Radiation, 2004, 11, 291-294.	2.4	6
304	An XAFS Study on the Polymer Protected CuPd Bimetallic Nanoparticles A Novel HeterobondPhilic Structure. Physica Scripta, 2005, , 781.	2.5	6
305	A new optical doping method toward molecular electronics. Synthetic Metals, 2005, 152, 289-292.	3.9	6
306	Growth of carbon nanofibers on nanoscale catalyst strips fabricated with a focused ion beam. Nanotechnology, 2008, 19, 405302.	2.6	6

#	Article	IF	CITATIONS
307	Anisotropic growth of a nickel trimer formed on a highly-stepped TiO2(110) surface. Chemical Physics Letters, 2013, 570, 64-69.	2.6	6
308	A new spectroelectrochemical cell forin situmeasurement of Pt and Au K-edge X-ray absorption fine structure. Review of Scientific Instruments, 2014, 85, 084104.	1.3	6
309	An Origin for Lattice Expansion in PVP-Protected Small Pd Metal Nanoparticles. Bulletin of the Chemical Society of Japan, 2017, 90, 720-727.	3.2	6
310	Polarized Total-Reflection Fluorescence EXAFS Studies on Asymmetric Surface Structures of Catalysts. Japanese Journal of Applied Physics, 1993, 32, 413.	1.5	6
311	Methylruthenium carbidocarbonyl clusters supported on inorganic oxides: characterization and selective acetaldehyde formation. Journal of the Chemical Society Dalton Transactions, 1992, , 2287.	1.1	5
312	Reversible Activity Enhancement of SiO2-Supported Group VIII Metal Catalysts by Pretreatment Temperature. Journal of Catalysis, 1993, 143, 22-31.	6.2	5
313	Formation of a stabilized coordinatively unsaturated metal carbonyl cluster, H2Ru4(CO)12, by photochemical reaction of H2Ru4(CO)13 adsorbed on the surface of silica. The Journal of Physical Chemistry, 1993, 97, 656-660.	2.9	5
314	Water-promoted oxygen isotope exchange on a Pt4+/MgO catalyst. Journal of the Chemical Society, Faraday Transactions, 1998, 94, 2639-2646.	1.7	5
315	Surface catalytic reactions assisted by gas phase molecules on supported Co-ensemble catalysts. Studies in Surface Science and Catalysis, 2000, 130, 605-610.	1.5	5
316	DXAFS study on the decarbonylation process of Mo(CO)6in NaY supercages. Journal of Synchrotron Radiation, 2001, 8, 628-630.	2.4	5
317	In Situ XRay Absorption Fine Structure Studies on the Structure of Ni2P Supported on SiO2. Physica Scripta, 2005, , 822.	2.5	5
318	Photochemical fabrication of molecular devices. Journal of Non-Crystalline Solids, 2006, 352, 2628-2630.	3.1	5
319	An approach to nano-chemical analysis through NC-AFM technique. Catalysis Today, 2006, 117, 80-83.	4.4	5
320	XAFS Analysis of Ti and Ni Dissolution from Pure Ti, Ni–Ti Alloy, and SUS304 in Soft Tissues. Chemistry Letters, 2008, 37, 958-959.	1.3	5
321	A high-temperature in situ cell with a large solid angle for fluorescence X-ray absorption fine structure measurement. Review of Scientific Instruments, 2015, 86, 034102.	1.3	5
322	Light and Shadow Effects in the Submerged Photolytic Synthesis of Micropatterned CuO Nanoflowers and ZnO Nanorods as Optoelectronic Surfaces. ACS Applied Nano Materials, 2020, 3, 1783-1791.	5.0	5
323	Development of <i>Operando</i> Polarization-Dependent Total Reflection Fluorescence X-ray Absorption Fine Structure Technique for Three-Dimensional Structure Determination of Active Metal Species on a Model Catalyst Surface under Working Conditions. Journal of Physical Chemistry C, 2021, 125. 12424-12432.	3.1	5
324	NEW "Pd / ULTRA-THIN AMORPHOUS-OXIDE LAYER /ZSM-5―CATALYSTS FOR SELECTIVE FORMATION OF PROPANE FROM CO/H2. Chemistry Letters, 1986, 15, 855-858.	1.3	4

#	Article	IF	CITATIONS
325	EXAFS studies about the mechanism of the CO oxidation reaction on the Co tetramer catalyst. Physica B: Condensed Matter, 1989, 158, 152-153.	2.7	4
326	Ni(II) Complexes ofN,N′-Ethylenebis(o-mercaptobenzamide): A Quadridentate Thiolato Amide {S2N2} Ligand. Bulletin of the Chemical Society of Japan, 1990, 63, 999-1004.	3.2	4
327	Wavelength dependent photochemical decarbonylation of H2Ru4(CO)13 to form coordinatively unsaturated H2Ru4(CO)12 in solid matrixes at 77 K: a model for the photoreaction postulated to form H2Ru4(CO)12 on the surface of silica. The Journal of Physical Chemistry, 1993, 97, 565-568.	2.9	4
328	Reversible structural change of Rh particles supported on GeO2 submonolayers–SiO2 in reduction and oxidation by XAFS, XRD, TEM and FTIR. Journal of the Chemical Society, Faraday Transactions, 1997, 93, 3217-3227.	1.7	4
329	Title is missing!. Topics in Catalysis, 2002, 20, 89-95.	2.8	4
330	Recent progress in energy-filtered high energy X-ray photoemission electron microscopy using a Wien filter type energy analyzer. Applied Surface Science, 2004, 237, 637-640.	6.1	4
331	Photochemical Method of Device Fabrication Starting from Molecular Crystals. Molecular Crystals and Liquid Crystals, 2006, 455, 311-316.	0.9	4
332	Portable ultrahigh-vacuum sample storage system for polarization-dependent total-reflection fluorescence x-ray absorption fine structure spectroscopy. Journal of Vacuum Science and Technology A: Vacuum, Surfaces and Films, 2016, 34, .	2.1	4
333	Development of Surface Fluorescence Xâ€Ray Absorption Fine Structure Spectroscopy Using a Laueâ€Type Monochromator. Chemical Record, 2019, 19, 1157-1165.	5.8	4
334	Tracking the Local Structure Change during the Photoabsorption Processes of Photocatalysts by the Ultrafast Pump-Probe XAFS Method. Applied Sciences (Switzerland), 2020, 10, 7818.	2.5	4
335	Energy Filtered X-Ray Photoemission Electron Microscopy. Advances in Imaging and Electron Physics, 2010, , 1-43.	0.2	4
336	Bent crystal Laue analyser combined with total reflection fluorescence X-ray absorption fine structure (BCLA + TRF-XAFS) and its application to surface studies. Journal of Synchrotron Radiation, 2020, 27, 1618-1625.	2.4	4
337	Micro Reverse Monte Carlo Approach to EXAFS Analysis. E-Journal of Surface Science and Nanotechnology, 2014, 12, 322-329.	0.4	4
338	EXAFS Studies on the Adsorption Structures of P/Ni(111). Japanese Journal of Applied Physics, 1993, 32, 359.	1.5	4
339	Synthesis of a linear-type pentanuclear (RhIII-WVI-CuI-WVI-RhIII) sulfide cluster predicted by fast atom bombardment mass spectrometry. Journal of Cluster Science, 1995, 6, 421-436.	3.3	3
340	Reversible structure change of one-atomic layer GeO2 on SiO2 surface under the interaction with Rh particles by in situ XAFS studies. Catalysis Today, 1998, 39, 343-350.	4.4	3
341	In situ energy-dispersive XAFS study of the reduction process of Cu-ZSM-5 catalysts with 1 s time-resolution. Studies in Surface Science and Catalysis, 2001, 132, 785-788.	1.5	3
342	Photochemical control of dark conductivity - a new approach to devices based on molecular crystals. Journal of Low Temperature Physics, 2006, 142, 383-386.	1.4	3

#	Article	IF	CITATIONS
343	In Situ EXAFS Studies on Ni2P Hydrodesulfurization Catalysts in the Presence of High Pressure and High Temperature Oil. AIP Conference Proceedings, 2007, , .	0.4	3
344	Electrodeposition Study on a Single-crystal Titanium Dioxide Electrode: Platinum on a Niobium-doped Titanium Dioxide(110) Electrode. Chemistry Letters, 2014, 43, 1797-1799.	1.3	3
345	Degradation mechanism of a high-performance real micro gas sensor, as determined by spatially resolved XAFS. Physical Chemistry Chemical Physics, 2016, 18, 7374-7380.	2.8	3
346	Evidence for Multi-Atom Resonance X-ray Raman Spectroscopy — An <i>in situ</i> Low <i>Z</i> -element and Bond-specific X-ray Spectroscopy. E-Journal of Surface Science and Nanotechnology, 2018, 16, 387-390.	0.4	3
347	Premodified Surface Method to Obtain Ultraâ€Highly Dispersed Metals and their 3D Structure Control on an Oxide Singleâ€Crystal Surface. Chemical Record, 2019, 19, 1244-1255.	5.8	3
348	What is the Origin for Peaks at the <i>L</i> ₃ XANES Spectra of AgCl?. E-Journal of Surface Science and Nanotechnology, 2012, 10, 609-612.	0.4	3
349	EXAFS Observation of Li Additive Effect on Structure of Rh Particles Supported on Zeolite. Japanese Journal of Applied Physics, 1999, 38, 81.	1.5	3
350	Abnormal Metal Bond Distances in PtAu Alloy Nanoparticles: <i>In Situ</i> Back-Illumination XAFS Investigations of the Structure of PtAu Nanoparticles on a Flat HOPG Substrate Prepared by Arc Plasma Deposition. Journal of Physical Chemistry C, 2022, 126, 1006-1016.	3.1	3
351	Constrained Thorough Search Analysis of Multi-edge EXAFS Spectra for Characterization of Bimetallic Nanoparticles. Chemistry Letters, 2022, 51, 538-541.	1.3	3
352	Molecular recognition of mannose-type aldoses by nickel(II) diamine complexes. An EXAFS study of Ni(II) complexes containing carbohydrates Nippon Kagaku Kaishi / Chemical Society of Japan - Chemistry and Industrial Chemistry Journal, 1987, 1987, 322-327.	0.1	2
353	EXAFS studies on molecular phenomena on solid catalysts in a working state. Physica B: Condensed Matter, 1989, 158, 142-144.	2.7	2
354	Self Terminating Reaction of Dipivaloylmethanate Complexes with Hydroxyl Groups on Oxide Surface. Materials Research Society Symposia Proceedings, 1991, 222, 333.	0.1	2
355	A local structure of P adsorbed on Ni(7 9 11) step surface. Physica B: Condensed Matter, 1995, 208-209, 465-466.	2.7	2
356	Metal Oxide Catalysts. Series on Synchrotron Radiation Techniques and Applications, 1996, , 192-215.	0.2	2
357	Chapter 5 Application to surface structure analyses. Analytical Spectroscopy Library, 1996, , 307-351.	0.1	2
358	Rh/One-atomic Layer GeO2/SiO2as a New Catalyst for Ethyl Acetate Hydrogenation at a Low Pressure. Chemistry Letters, 1997, 26, 985-986.	1.3	2
359	Three dimensional analysis of the local structure of Cu on TiO2(110) by in-situ polarization-dependent total-reflection fluorescence XAFS. Studies in Surface Science and Catalysis, 2001, 132, 757-760.	1.5	2
360	Photochemical Control of Dark Conductivity - A New Approach to Devices Based on Molecular Crystals. Journal of Low Temperature Physics, 2007, 142, 387-390.	1.4	2

#	Article	IF	CITATIONS
361	A Demonstration of Pt L3-Edge EXAFS Free from Au L3-Edge Using Log–Spiral Bent Crystal Laue Analyzers. Catalysts, 2018, 8, 204.	3.5	2
362	EXAFS study of Ti0.98Pd0.02O2-δ catalyst. AIP Conference Proceedings, 2018, , .	0.4	2
363	Theory of multi-atom resonant Raman scattering. Journal of Electron Spectroscopy and Related Phenomena, 2019, 233, 57-63.	1.7	2
364	X-ray absorption fine structure studies on nickel phosphide catalysts for the non-oxidative coupling of methane reaction using a theoretical model. Radiation Physics and Chemistry, 2021, 189, 109727.	2.8	2
365	Structure and Bonding of Trace Ni Catalyst in Carbon Nanotube Studied by Ni K-Edge XANES. E-Journal of Surface Science and Nanotechnology, 2005, 3, 427-432.	0.4	2
366	Approach to Highly Sensitive XAFS by Means of Bent Crystal Laue Analyzers. Hyomen Kagaku, 2017, 38, 378-383.	0.0	2
367	Structure of Dipivaloylmethanate Complexes Adsorbed with Hydroxyls on SiO2Surface by EXAFS. Japanese Journal of Applied Physics, 1993, 32, 431.	1.5	2
368	Surface reaction induced by FEL-IR. Japanese Journal of Applied Physics, 2002, 41, 118.	1.5	2
369	Principles Pertaining to the Metal-support Interaction on Metal Oxide Surfaces. Hyomen Kagaku, 2009, 30, 84-91.	0.0	2
370	EXAFS AND XANES STUDIES ON THE LOCAL STRUCTURES OF METAL IONS IN METAL DOPED MgO SYSTEMS. Journal De Physique Colloque, 1986, 47, C8-317-C8-320.	0.2	1
371	EXAFS Study on One-Dimensional Halogen-Bridged Mixed-Metal (Pd, Pt)Mixed-Valence Complexes. Bulletin of the Chemical Society of Japan, 1986, 59, 3271-3272.	3.2	1
372	Chemical Control of Noble Metal Catalysis by Main Group Elements. Materials Research Society Symposia Proceedings, 1997, 497, 99.	0.1	1
373	A novel effect of Li additive: dynamic control of Rh mobility during CO2 hydrogenation reaction. Studies in Surface Science and Catalysis, 2000, 130, 3759-3764.	1.5	1
374	Full Multiple Scattering Analyses of Pt L-edge XANES for CO/pt Clusters Hyomen Kagaku, 2001, 22, 517-521.	0.0	1
375	Polarization Dependent Total Reflection Fluorescence XAFS Studies on Interface Structures between Metal and Oxide Substrate. Hyomen Kagaku, 2002, 23, 332-338.	0.0	1
376	Studies on Surface and Interface with X-ray Absorption Fine Structure (XAFS). Time Resolved XAFS Studies for Catalysts Preparation Hyomen Kagaku, 2002, 23, 339-344.	0.0	1
377	Time-Resolved DXAFS Study of Adsorption and Release of Hydrogen on Pt/MCM-41. AIP Conference Proceedings, 2007, , .	0.4	1
378	Improvement of the XANAM System and Acquisition of a Peak Signal with a High S/N ratio. Journal of Physics: Conference Series, 2007, 61, 1117-1121.	0.4	1

#	Article	IF	CITATIONS
379	Preparation of Well-defined Inhomogeneous ^ ^alpha;-Sb2O4/VSbO4 Catalyst by Electron Lithography and their Catalytic Activities. Hyomen Kagaku, 2012, 33, 426-430.	0.0	1
380	Reactivity of Ni2P(10-10) Surface for NO Evaluated by STM. Hyomen Kagaku, 2014, 35, 415-419.	0.0	1
381	X-Ray Absorption Fine Structure Analysis of Catalytic Nanomaterials. , 2016, , 609-664.		1
382	Dynamics of Photoelectrons and Structural Changes of Tungsten Trioxide Observed by Femtosecond Transient XAFS. Angewandte Chemie, 2016, 128, 1386-1389.	2.0	1
383	Controlling the inhomogeneity of solid catalysts at the mesoscopic scale. Chemical Physics Letters, 2017, 683, 18-21.	2.6	1
384	Three-Dimensional Structures on Oxide Single-Crystal Surfaces. , 2017, , 527-538.		1
385	A new interpretation of the â^š7×â^š7 R19.1° structure for P adsorbed on a Ni(111) surface. Science and Technology of Advanced Materials, 2019, 20, 379-387.	6.1	1
386	Extracting the local electronic states of Pt polycrystalline films surface under electrochemical conditions using polarization-dependent total reflection fluorescence x-ray absorption near edge structure spectroscopy. Electronic Structure, 2020, 2, 044003.	2.8	1
387	Angle-Resolved and Resonant Photoelectron Spectroscopy Study of Ni2P (10-10) Single-Crystal Surface. Hyomen Kagaku, 2010, 31, 324-330.	0.0	1
388	Special Issue on Recent Developments of the Study on Catalytic Reaction Mechanisms. Direct Observation of Spatiotemporal Patterns on Pt Surface and Its Chemical Control Hyomen Kagaku, 1996, 17, 194-200.	0.0	1
389	Temperature-Dependent XAFS Study on AgBr1-xlxSolid Solution. Japanese Journal of Applied Physics, 1993, 32, 640.	1.5	Ο
390	Development of a Multi Surface Imaging System for LEEM, PEEM, SEEM, AEEM and XPEEM. Hyomen Kagaku, 1998, 19, 498-502.	0.0	0
391	Hydrogenation of CO2 over Rh ion exchanged zeolite catalysts. Studies in Surface Science and Catalysis, 1998, , 455-458.	1.5	Ο
392	XAFS Study on the Structure of Mo Species in NaY Zeolite Derived from Mo(CO)6. Japanese Journal of Applied Physics, 1999, 38, 85.	1.5	0
393	Ni K-Edge XANES Analyses of Residual Ni Catalyst in Carbon Nanofiber Using Full Multiple Scattering Theory. AIP Conference Proceedings, 2007, , .	0.4	Ο
394	A New Collinear-Type Energy-Filtered X-ray Photoemission Electron Microscope Equipped with a Multi-Pole Aberration-Corrected Air-Core Coil Wien Filter. Japanese Journal of Applied Physics, 2012, 51, 046701.	1.5	0
395	New Prospects for the Characterization of Heterogeneous Catalysts by Using Slow Muon Spectroscopy. , 2014, , .		0
396	Special Issue on Surface Science. Chemical Record, 2014, 14, 756-758.	5.8	0

#	Article	IF	CITATIONS
397	The 16th International Symposium on Relations Between Homogeneous and Heterogeneous Catalysis (ISHHC-16), Sapporo, August 4–9, 2013. Topics in Catalysis, 2014, 57, 811-811.	2.8	0
398	Nanostructures and Properties of Rutile TiO ₂ Studied by Accelerator-based Probes. Nihon Kessho Gakkaishi, 2015, 57, 41-46.	0.0	0
399	XAFS for Ultra Dilute Systems. , 2017, , 193-206.		0
400	Ultra-Fast XAFS Studies on Photocatalyst Using SACLA. Nihon Kessho Gakkaishi, 2017, 59, 24-28.	0.0	0
401	Key Technologies for Next Generation Thin Film Silicon Solar Cells. Polarization-Dependent Total Reflection Fluorescence EXAFS Study on the 3-Dimensional Structural Analysis of Surface Active Sites Hyomen Kagaku, 2000, 21, 294-299.	0.0	0
402	OS8-1-4 Experimental Study on Pressure Loss of Horizontal Core-Annular Flow. The Abstracts of ATEM International Conference on Advanced Technology in Experimental Mechanics Asian Conference on Experimental Mechanics, 2007, 2007.6, _OS8-1-4-1OS8-1-4-6.	0.0	0
403	Vacuum and Environmental Catalysts. Journal of the Vacuum Society of Japan, 2010, 53, 19-24.	0.3	0
404	A New Collinear-Type Energy-Filtered X-ray Photoemission Electron Microscope Equipped with a Multi-Pole Aberration-Corrected Air-Core Coil Wien Filter. Japanese Journal of Applied Physics, 2012, 51, 046701.	1.5	0
405	EXAFS and XANES Studies of FeCl3-Doped Polyacetylenes. Springer Proceedings in Physics, 1984, , 392-393.	0.2	0
406	In-laboratory EXAFS apparatus by use of plane-crystal monochromator Nihon Kessho Gakkaishi, 1985, 27, 209-213.	0.0	0
407	SEXAFS Studies of Sulfur Adsorbed on a Nickel Stepped Surface. Japanese Journal of Applied Physics, 1993, 32, 365.	1.5	0
408	Reversible Deformation of SiO ₂ -Supported PtAu ₆ Cluster Induced by the CO Adsorption by In Situ EXAFS. European Physical Journal Special Topics, 1997, 7, C2-863-C2-865.	0.2	0
409	The Interaction between Hydrogen and Palladium Studied by XANES Spectra Hyomen Kagaku, 1998, 19, 486-490.	0.0	0
410	Ultra-high Dispersion of Metals on an Oxide Single-crystal Surface Premodified with a Functional Organic Molecule and Their 3D Structure Analysis by PTRF-XAFS Technique. Vacuum and Surface Science, 2018, 61, 309-314.	0.1	0
411	Solving Energy and Environmental Challenges with Synchrotron Radiation Technology. Synchrotron Radiation News, 2020, 33, 2-3.	0.8	0
412	Ce K-EDGE EXAFS SPECTRUM OF CeO2. Journal De Physique Colloque, 1986, 47, C8-185-C8-188.	0.2	0
413	Angular Dependence of Multi-atom Resonant X-ray Raman Scattering. E-Journal of Surface Science and Nanotechnology, 2022, , .	0.4	0